

# Ibn Al-Haitham Journal for Pure and Applied Sciences

Journal homepage: jih.uobaghdad.edu.iq PISSN: 1609-4042, EISSN: 2521-3407 IHJPAS. 2025, 38(4)



# Effect of Cerium Ion on Microstructure and Dielectric Properties of Ni-Zn Ferrites Prepared by Solid State Reaction Method

Amna M. Hitler<sup>1</sup> ■ and Abbas K. Saadon<sup>2\*</sup> ■

<sup>1,2</sup> Department of Physics, College of Education for Pure Science (Ibn-ALHaitham), University of Baghdad, Baghdad. Iraq
\*Corresponding Author

Received:16 January 2025 doi.org/10.30526/38.4.4109

Accepted:6 May 2025

Published:20 Octoper 2025

#### Abstract

In this work, the Nickel and zinc Ferrite Ni<sub>0.5</sub>Zn<sub>0.5</sub> Fe<sub>2</sub>O<sub>4</sub> +XCeO<sub>2</sub> in purity and purity structure were prepared at multi–concentration X (0.0,0.05,0.10,0.15, and 0.20) using the solid state interaction method at a temperature (1000 °C) for four hours in air. The XR-diffraction shows that the prepared powder samples have a spinal structure at single cubic phase. The lattice parameters were decreasing from 8.331 to 8.3021 with increasing concentration of cerium's Ionic Ce<sup>4+</sup>, also the crystal volume for purity samples is larger than in purity samples, decreasing from (578.217 to 571.993) A°3 with increasing concentration. However, the real and imaginary dielectric constants were measured for both pure and in purity samples by Ce<sup>4+</sup>. The dielectric constant shows that up to down decreases with increasing frequency. However, the x-ray density was increasing from 6.887 g/cm³ to 6.963 g/cm³ with increasing concentration. The conductivity of alternating current for preparing the sample increased firstly with frequency and remained constant, then a constant behavior was observed at higher frequencies. The microscopic pharmaology structure using the tunneling electron microscopy, that which particles have a spherical structure.

**Keywords:** Mixed ferrite, Dielectric constant, Microstructure, Rare-earth doping.

#### 1. Introduction

Recently, the manufacture of Nickel Ni and Zinc Zn Ferrites, that's mixed with earth rare, has become more interesting to more researchers in the Global Country. N. Arundhati and D. Ravinder. The sol-gel method was used to prepare crystalline nanomaterials from Ni  $Ce_x Fe_{2-x}O_4$  (x=0.0-0.04 with a difference 0-0.010). The crystalline phase of the prepared sample was shown by diffraction, and the crystal Size was calculated using the Debye-Scherrer method to be (14-26 nm). The particle Properties were also studied, and the results of AC conductivity, impedance (Z), dielectric constant ( $\dot{\epsilon}$ ), and loss factor (tan  $\delta$ ) were analyzed. There is an increase in the( $\sigma$ Ac) of the sample with increasing temperature and additive Concentration, and the dielectric constant and loss decrease with increasing frequency. The Ni and Zn-Ferrites is one important branch because the higher Saturation magnetic and less dielectric loser in additionally, the adding of rare earth elements to Ni and Zn molecules leads to enhance The electric characteristic and used in high frequency applicable and magnetic ram (1), the preparing of Ni and Zn molecules methods have much Important to obtain good

characteristics for Ferrite particles in morphology and micro structure (2). It was reported various properties of nickel and zinc ferrites by (3). The volatilization of zinc at high temperatures produces iron ions, which increases the electron mobility and reduces the resistance of Nickel-Zinc ferrite. Aswell as it was studied the AC resistance and dielectric transport properties of Nickel-Zinc ferrites prepared by Conventional ceramic technology by (4). The replacement of rare earth ions in nickel-zinc ferrite was investigated, where the replacement of Fe<sup>3+</sup> with rare earth ions resulted in a reduction in the solubility of the spinel lattice due to its large ionic diameters (5). The Cerium element has a multi-chemical structure that allows it to be used in different applications and Various oxide states to produce good magnetic behavior, resulting in a change in the structure of the Ferrite lattice. In the past years, the rare earth elements used in recharging batteries, photo emission diode, solar cells, and superconductivity in different fields, these elements are called fundamentally advanced industrial (6). In the present work, we investigated the effect of Ce<sup>4+</sup> on microstructure and electric properties for Ni, Zn-ferrites by adding many different Ce<sup>4+</sup> concentrations.

### 2. Materials and Methods

The Ni<sub>0.5</sub> Zn<sub>0.5</sub> Fe<sub>2</sub>O<sub>4</sub>+ X CeO<sub>2</sub> was prepared at X = (0.0,0.05, 0.10, 0.15, and 0.20) using solid state reaction methods by mixing the oxides (NiO, ZnO, Fe<sub>2</sub>O<sub>4</sub>, and CeO<sub>2</sub>, These oxides are fundamental materials in preparing Ferrite; the NiO, ZnO, Fe<sub>2</sub>O<sub>4</sub>, and CeO<sub>2</sub> oxides are mixed in an ethanol solvent medium. Next, the produced Powder was heated at (1000°C) for 4 hours in air. The powders are formed into multi-disc samples at a thickness (3mm and 1.5cm diameter using hydraulic Compressors. All samples were heated at (1000°C) for 5hours. The crystal morphology and crystal structure for preparing samples after sintering using XR-diffraction using light have been ( $\lambda$ =1.5418 A°) Cu- $K_{\alpha}$ The micro morphology test and the structure were analyzed using the Scanning Electron Microscopy (SEM). Furthermore, the surfaces Samples made smooth and painted the surface by Ag paste, with drying at 100°C for ½ hrs. to measure the electricity parameters for preparing samples. The dielectric measurement is performed on all samples using an LCR-meter, on the results of measuring the real and imaginary dielectric constant are taken at (50Hz to 1MHz).

#### 3. Results and Discussion

The pattern of XR-diffraction for Ni-Zn Ferrite structure in two state pure and mixed with  $Ce^{4+}$  at Concentration X= (0.0,0.05,0.10,0.15, and 0.20) The peak of XR-diffraction agrees with plane reflection for spinal Cubic Crystal of Ni and Zn Ferrite were shwen in **Figure 1.** 

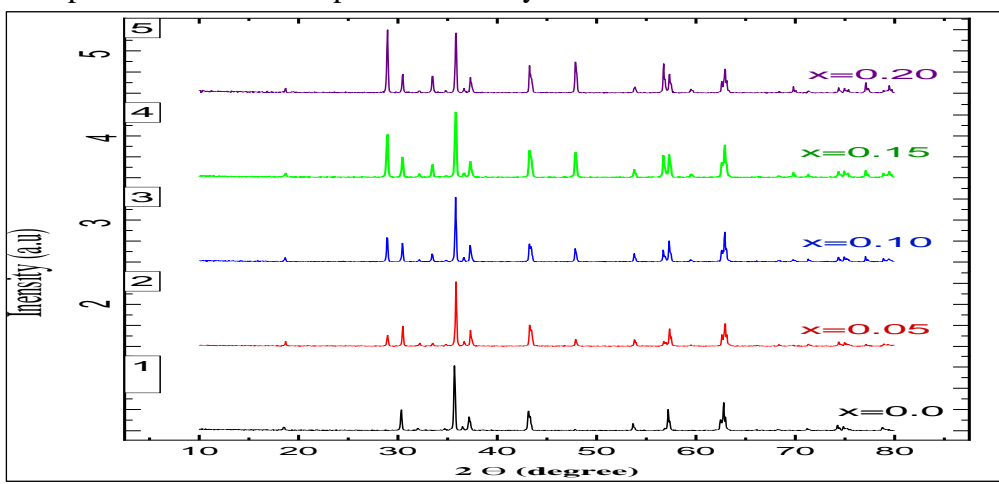


Figure 1. XRD Patterns of Ni-ZnFe<sub>2</sub>O<sub>4</sub>+XCeO<sub>2</sub>.

From **Figure 1**, we can show the crystallites will be decreasing with increasing of Ce<sup>4+</sup> Concentration because decreasing the probity density in noted peaks. we also notice from the figure (1) the Cubic Structure of nickel-Zinc ferrite, as a Secondary phase called CeO<sub>2</sub> appeared in the levels (111), (200), (220) these results were obtained from matching with cerium oxide CeO<sub>2</sub> Jcpps 00-001-0800. This may be because the added substance has an ionic radius of (1.034 A°) larger than the host (0-64 A°) where the higher radius Ce<sup>4+</sup> prevents replacement Fe<sup>3+</sup> and ther fore the sample with the higher Concentration Contains trace of Cerium. oxide. The XRD shows reflection Peaks (111), (022), (113) (222), (004), (224), (333), (044)-Indexed using a standard data set-Results obtained from the diffraction Pattern indexed with card number JCPDS 98-018-1847 corresponding to Ni-Zn Ferrite.

In addition, we show the height of peaks must be decreasing with increasing the Concentration of  $Ce^{4+}$  Ionic, the peak beach to minimum at (x=0.20), The lattice Constants be decreasing while the crystal volume decreasing to down with increasing the concentration of  $Ce^{4+}$  for preparing samples,

Cerium element has an ionic radius (1.11A°) and therefore it is difficult to insert into the unit cell of the Nickel-Zinc ferrite spinel lattice, therefore, from the solubility limit of cerium ions in the unit cell of the Nickel-Zinc ferrite is  $X \approx 0.05$  therefore the cerium ion needs a high activation energy to displace the Fe³+ ion to enter the octahedral B sites ,where the binding energy of (Ce-O) is higher camped to the binding energy of (Fe-O) this means that the formation and growth of nickel-zinc ferrite doped with cerium ions requires a higher energy than that of pure nickel –Zinc ferrite therefore ,instead of occupying the Fe³+ sites in the lattice ,the Ce⁴+ ions enter the interstitial sites of the lattice ,which leads to an inconsistency in the structure of the samples, which stimulates the tariation of the crystalline properties ,and the lattice stress increases with increasing the concentration of Ce⁴+ ions and reduces the unit cell size that's agree with measuring in both literateness in (7,8,19,20 and 22).

The real and imaginary dielectric Constants. Were measuring tangent angle losses with conductivity of alternative current for all preparing Samples were measuring for Ni, Zn ferrite in both state pure and mix with Ce<sup>4+</sup> at frequency range (50Hz-1MHz) show the Figures (2), (3), (4) and (5), it can be noted that real and imaginary dielectric constant will be decreasing with increasing the low frequency and stay constant at high frequency that's agree with experiment results (7-9, 19, 21, 22).

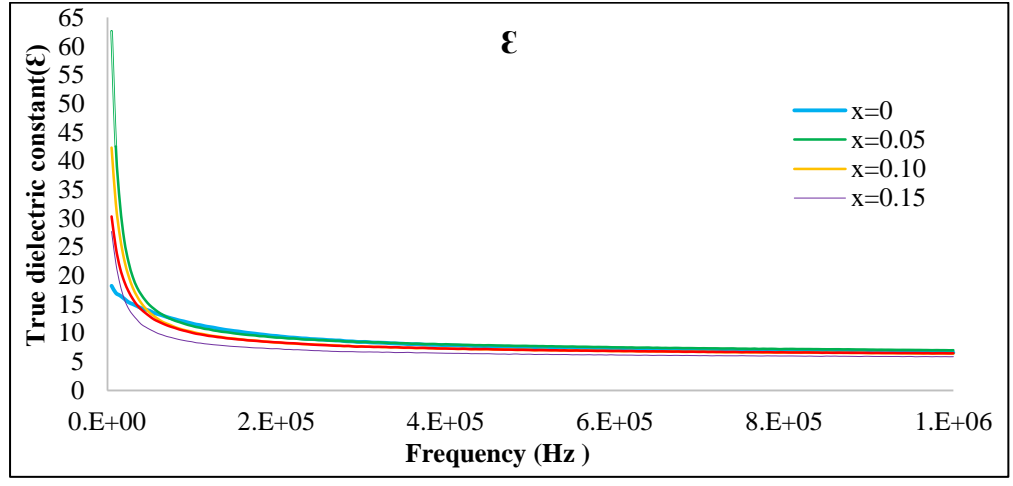


Figure 2. Change of real Dielectric constant with Frequency.

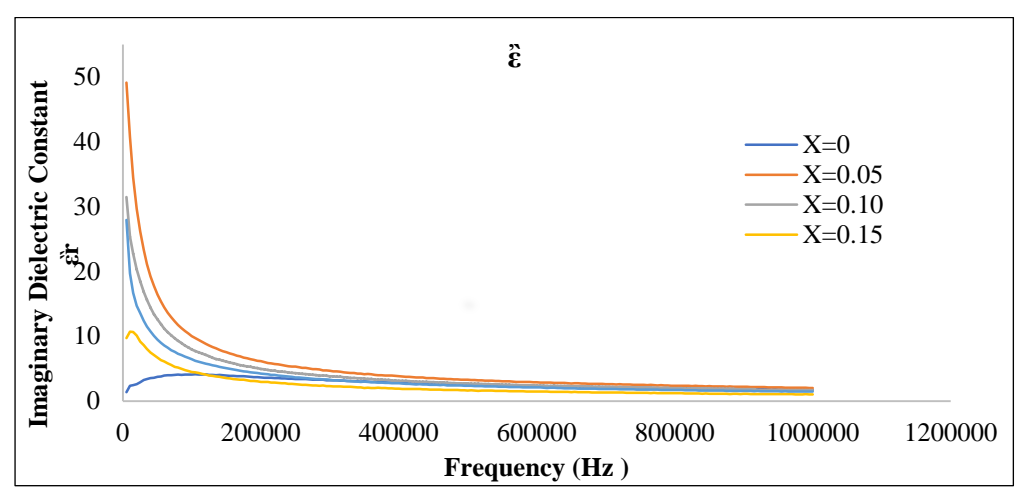


Figure 3. Change of imaginary Dielectric constant with frequency.

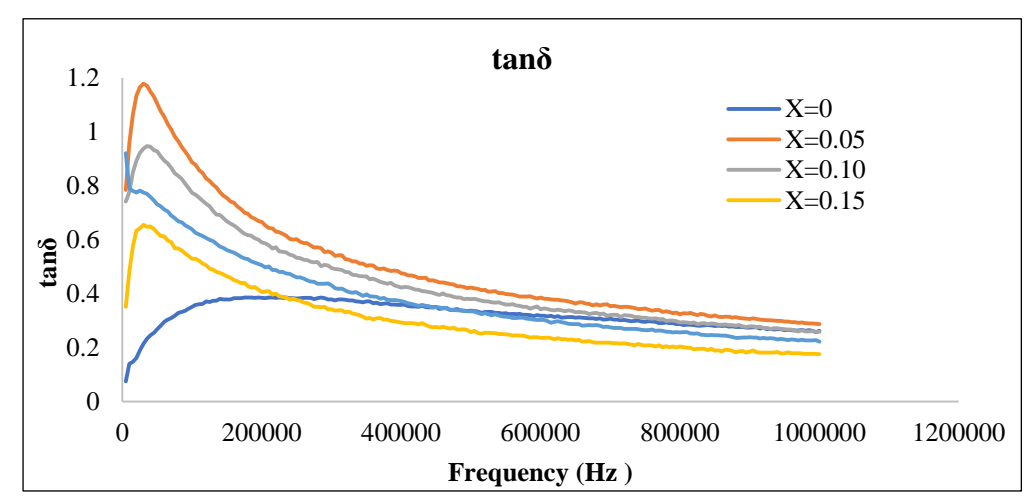


Figure 4. Change of tangent angle loss with frequency.

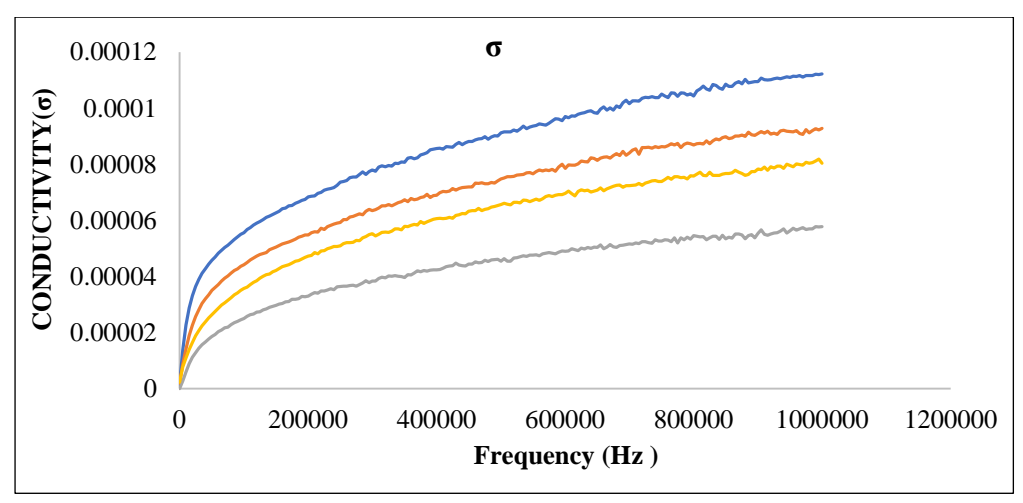


Figure 5. Change of Ac conductivity with frequency.

This indicated that electric polarized occurs under the electric field of alternating current. The permittivity (real dielectric) depends on the conductivity phenomena that occur due to electron transfer between Fe<sup>2+</sup> and Fe<sup>3+</sup> ions. The electron transfer leads to polarize at the grain boundary because electrons accumulate at the grain boundary as results in large resistance of grain boundaries (10, 11, 23-25).

The inter of Ce<sup>4+</sup> ions in the edge surface to change the position of Fe<sup>3+</sup> ions leads to a decrease in the electron transfer rate and to resist the Conductivity process. The specific

permittivity stays Constant due to a delay in the electron transfer process because of the change in the applied electric field.

On the other hand, the conductivity of alternative Current linear increases with low frequency because the electronic transfer process between Fe<sup>3+</sup> and Fe<sup>2+</sup> ionic that's have different equivalent states, and electron transfer between A and B sites is mainly important compared with electron transfer between B sites. As the increases in applied electric field increases, the electron transfer increases. And increases in conduction of alternative current (12-14, 26, 27). The Analysis of Scanning Electron Microscope SEM in **Figure 6** (A, B, C, D, and E).

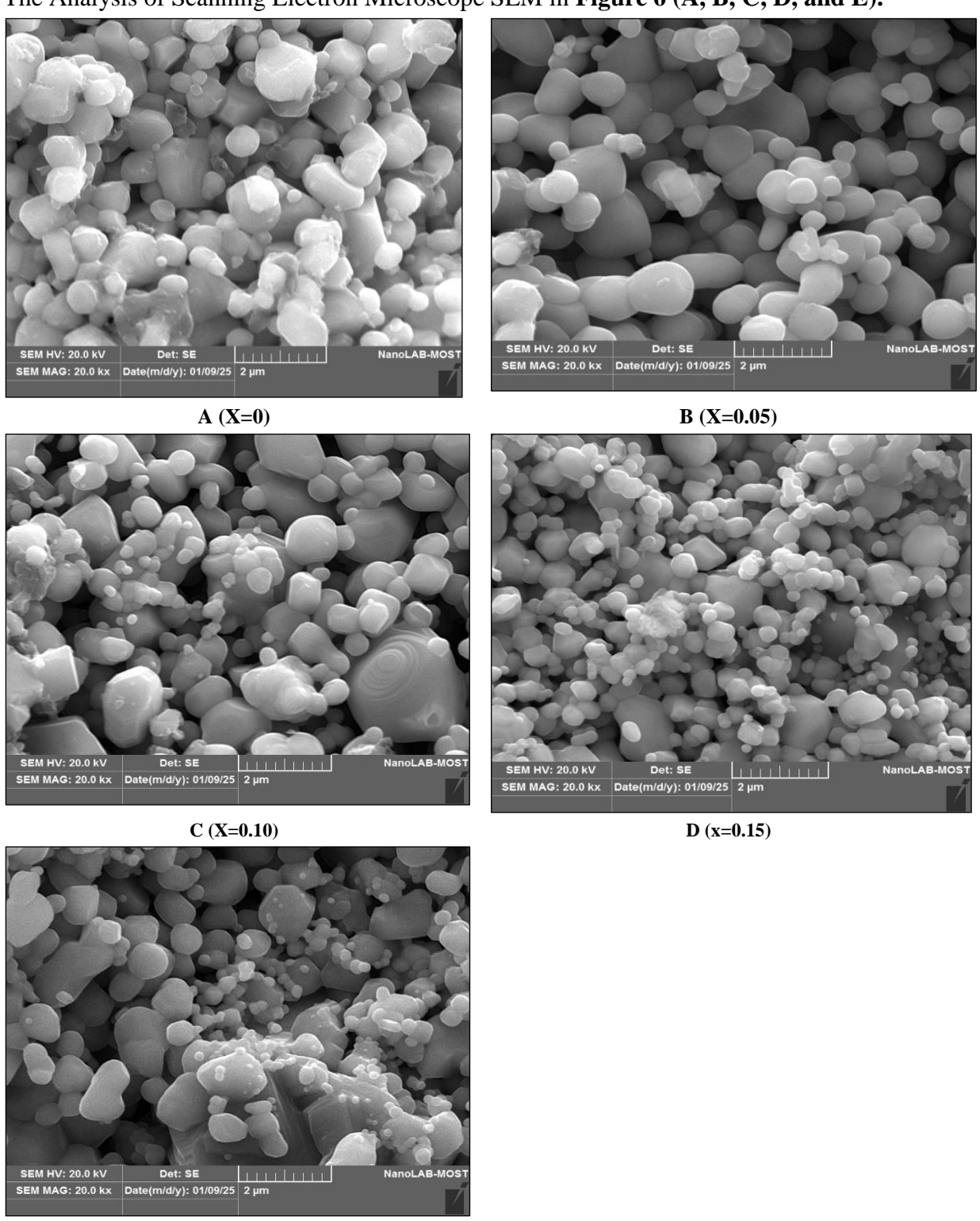


**Figure 6. A ,B, C, D, E** SEM images of  $Ni_{0.5} Zn_{0.5} Fe_2O_4 + XCeO_2$ .

E(x=0.20)

The show the product spherical particles and catalysts. The reason for the agglomerated structure is due to electrostatic attraction and Polarization of (cexNi Zn  $Fe_2O_4$ ).

The shape and volume of grain particles of Ferrite limited and effected on electric and structural characteristic of Ni, Zn Ferrite (15, 16, 28-30).

Look at the **Table 1** structure Parameter of  $Ni_{0.5}$   $Zn_{0.5}$   $Fe_2O_4+XCeO_2$  Samples. We can discuss the data in terms of change in values When composition x=(0,0.05,0.10,0.15 and 0.20) where the value of lattice constant (a) decrease gradually with compositions(X) from 0.0 to 0.20.

This indicates the effect of the introduction of the crystal lattice of Fe<sub>2</sub>O<sub>4</sub>, which be may due to the replacement of large ions with smaller ones. Unit cell volume The cell size also gradually decreases with increasing, which is consistent with the decrease in the lattice constant (31).

This reflects a reduction in the crystal lattice with increasing CeO<sub>2</sub> content.

Bulk density The bulk density initially decreases slightly from (3.496 at t to 3.328), then starts to increase at 3.379.

This can be explained by the transformations in the crystal structure and the effect of the gradual introduction of CeO<sub>2</sub>.

X-ray density: X-ray diffraction increases very slightly with increasing, which may be due to redistribution of ions within the crystal lattice.

The particle size shows a decreasing trend with increasing x (with cerium concentration)

- -At (X=0.0): 475.2 nm.
- -At(X=0.05) :600.16 nm (clear increase).
- With further increase X, the grain size decreases to 188.66 nm at (X=0.20).

This can be explained by the fact that the addition of CeO<sub>2</sub> initially increases the growth rate of the grains and then leads to a reduction in their size due to the restrictions resulting from the introduction of CeO<sub>2</sub>.

Table 1	L. structure	Parameter	1 to	$N1_{0.5}$	$Zn_{0.5}$	Fe <sub>2</sub> o <sub>4</sub> +.	XCe(	$J_2$ Samples	3.
---------	--------------	-----------	------	------------	------------	-----------------------------------	------	---------------	----

Compositions (x)	Lattice	Unit cell	Bulk density	x-ray density	Grain size
	constant $a(A^{\circ})$	volume V(A°3)	$\rho_{\rm B}({ m g/cm}^3)$	$\rho_{\rm x}({\rm g/cm}^3)$	(nm)
0.0	8.331	578.217	3.496	6.887	475.2
0.05	8.308	573.441	3.354	6.945	600.16
0.10	8.306	573.027	3.328	6.950	258
0.15	8.305	572.820	3.379	6.953	232.66
0.20	8.301	571.993	3.462	6.963	188.66

#### 4. Conclusion

In concluded, we find the adding various of concentration  $Ce^{4+}$  to Ni, Zn Ferrite Ni<sub>0.5</sub> Zn<sub>0.5</sub>, Fe<sub>2</sub>O<sub>4</sub> + X CeO<sub>2</sub> at x = (0, 0.05, 0.10, 0.15 and 0.20) are large changing in Ni, Zn Ferrites properties. The lattice constants and crystal Volume decreases with increasing  $Ce^{4+}$  Ionic also that Increasing in porosity. This indicated that Ni and Zn Ferrites with  $Ce^{4+}$ , Can be used a good adsorption material. On the other hand, the decreases in dielectric constant at low frequency for samples with  $Ce^{4+}$  because decrease the of the electron transfer rate to exchange  $Ce^{4+}$  in eight edge surfaces and recharge the position of  $Fe^{3+}$  ions.

### Acknowledgment

Not applicable.

#### **Conflict of Interest**

The authors declare that they have no conflicts of interest.

#### **Funding**

The authors received no financial support for the research, authorship, and/or publication of this article.

### **Ethical Clearance**

The study did not involve human participants, animal subjects, or any form of personal data collection. Therefore, ethical approval and informed consent were not required.

#### References

- 1. Lide DR, editor. CRC handbook of chemistry and physics. CRC Press; 2004.
- 2. Sreematha B, Arundhatha N, Ravinder D. Influence of cerium substitution on structural, optical, and electrical transport properties of Ni-nano ferrites prepared by citrate gel auto-combustion method. Results Chem. 2023;5:100029. <a href="https://doi.org/10.1016/j.rechem.2023.100929">https://doi.org/10.1016/j.rechem.2023.100929</a>.
- 3. Shan M, Ding S, Hna J, Cui W, Wang W. Effect of annealing temperature on structural and magnetic properties of sol-gel synthesized Co0.8Fe2.2O4/SiO<sub>2</sub> nanocomposites. J Sol-Gel Sci Technol. 2018;88(3):53–60. https://doi.org/10.1007/s10971-018-4789-5.
- 4. Chandamma N, Manohara BM, Ujjinappa BS, Shankarmurthy GJ, Kumar MS. Structural and electrical properties of zinc-doped nickel ferrite nanoparticles prepared via a facile combustion technique. J Alloys Compd. 2017;702: 479-488. <a href="https://doi.org/10.1016/j.jallcom.2016.12.392">https://doi.org/10.1016/j.jallcom.2016.12.392</a>.
- 5. Akhtar MN, Yousaf M, Lu Y, Khan MA, Sarosh A, Arshad M, Niamat M, Farhan M, Ahmad, A, Khallidoon MU. Physical, structural, conductive and magneto-optical properties of rare earth (Yb, Gd) doped Ni–Zn spinel nanoferrites for data and energy storage devices. Ceram Int. 2021;47(9):11878–11886. https://doi.org/10.1016/j.ceramint.2021.01.028.
- 6. Kilbourn BT. Cerium and cerium compounds. Kirk-Othmer Encycl Chem Technol. 2000. https://doi.org/10.1002/0471238961.0305180911091202.a01
- 7. Haxel G. Rare earth elements: critical resources for high technology. US Dep Interior US Geol Surv; 2002.
- 8. Wang Y, Wu X, Zhang W, Chen W. Synthesis and electromagnetic properties of La-doped Ni–Zn ferrites. J Magn Magn Mater. 2016;398:90–95. https://doi.org/10.1016/j.jmmm.2015.09.044
- 9. Koops CG. On the dispersion of resistivity and dielectric constant of some semiconductors at audiofrequencies. Phys Rev. 1951;83(1):121–127. <a href="https://doi.org/10.1103/PhysRev.83.121">https://doi.org/10.1103/PhysRev.83.121</a>
- 10.Saadon AK. Preparation and study of some electrical properties of Mn–NiFe<sub>2</sub>O<sub>4</sub>. Ibn Al-Haitham J Pure Appl Sci. 2013;26(3):69–76. <a href="https://jih.uobaghdad.edu.iq/index.php/j/article/view/414">https://jih.uobaghdad.edu.iq/index.php/j/article/view/414</a>.
- 11.Saadon AK. Studying the effect of zirconia on some physical properties of porcelain. Ibn Al-Haitham J Pure Appl Sci. 2016;29(3):46–53. https://jih.uobaghdad.edu.iq/index.php/j/article/view/11.
- 12.Rezlescu N, Rezlescu E. Dielectric properties of copper-containing ferrites. Phys Status Solidi A. 1974;23(2):575–582. https://doi.org/10.1002/pssa.2210230229
- 13.Jassim KA, Hussein HS. Effect of partial substitution of lanthanum (La) on the structural and electric properties of Bi2Sr2Ca2Cu3-xLaxO10+δ. Ibn Al-Haitham J Pure Appl Sci. 2017;30(3):35–43. https://doi.org/10.30526/30.3.1600
- 14.Irvine JT, Huanosta A, Valenzuela R, West AR. Electrical properties of polycrystalline nickel zinc ferrites. J Am Ceram Soc. 1990;73(3):729–732. <a href="https://doi.org/10.1111/j.1151-2916.1990.tb06580.x">https://doi.org/10.1111/j.1151-2916.1990.tb06580.x</a>
- 15. Saadon AK, Shaban AH, Jasim KA. Effects of ferrite addition on the properties of polyethylene terephthalate. Baghdad Sci J. 2022;19(1):208. <a href="http://dx.doi.org/10.21123/bsj.2022.19.1.0208">http://dx.doi.org/10.21123/bsj.2022.19.1.0208</a>.
- 16.Jumaah DH, Saadon AK. Prepared and measuring the structural and dielectric properties of PbTiO3 and PdZrO3. AIP Conf Proc. 2019;2123(1). https://doi.org/10.1063/1.5116983.
- 17. Aleabi SH, Watan AW, Salman EM, Jasim KA, Shaban AH, AlSaadi TM. The study effect of weight fraction on thermal and electrical conductivity for unsaturated polyester composite alone and hybrid. AIP Conf Proc. 2018;1968(1). https://doi.org/10.1063/1.5039178.

- 18.Al-Khafaji RS, Jasim KA. Dependence of the microstructure specifications of earth metal lanthanum La substituted  $Bi2Ba_2CaCu_2-xLaxO_8+\delta$  on cation vacancies. AIMS Mater Sci. 2021;8(4): 550-509. https://doi.org/10.3934/matersci.2021034.
- 19. Sherin JJ, Bessy TC, Asha S, Kumar CV, Huessien D, Bindhu MR, Rasheed RA, Alarjani KM. Microwave-assisted hydrothermally synthesized cobalt-doped zinc ferrite nanoparticles for the degradation of organic dyes and antimicrobial applications. Environ Res. 2022;208:112687. <a href="https://doi.org/10.1016/j.envres.2022.112687">https://doi.org/10.1016/j.envres.2022.112687</a>.
- 20.Rahman MM, Hasan N, Hoque MA, Hossen MB, Arifuzzaman M. Structural, dielectric, and electrical transport properties of Al3+ substituted nanocrystalline Ni–Cu spinel ferrites prepared through the sol–gel route. Results Phys. 2022;38:105610. <a href="https://doi.org/10.1016/j.rinp.2022.105610">https://doi.org/10.1016/j.rinp.2022.105610</a>.
- 21.Akhtar MN, Yousaf M, Lu Y, Khan MA, Sarosh A, Arshad M, Niamat M, Farhan M, Ahmad A, Khallidoon MU. Physical, structural, conductive and magneto-optical properties of rare earths (Yb, Gd) doped Ni–Zn spinel nanoferrites for data and energy storage devices. Ceram Int. 2021;47(9):11878–11886. https://doi.org/10.1016/j.ceramint.2021.01.028.
- 22. Somvanshi SB, Jadhav SA, Khedkar MV, Kharat PB, More SD, Jadhav KM. Structural, thermal, spectral, optical and surface analysis of rare earth metal ion (Gd3+) doped mixed Zn–Mg nanospinel ferrites. Ceram Int. 2020;46(9):13170–13179. <a href="https://doi.org/10.1016/j.ceramint.2020.02.091">https://doi.org/10.1016/j.ceramint.2020.02.091</a>.
- 23.Goud S, Venkatesh N, Kumar DR, Barapati S, Veerasomaiah P. Study of structural, optical, photocatalytic, electromagnetic, and biological properties of Co0.75Mg0.25CexFe2-xO4 Mg-Co nanoferrites. Inorg Chem Commun. 2022;145:109969. https://doi.org/10.1016/j.inoche.2022.109969.
- 24. Sumalatha E, Edukondalu A, Ravinder D. Effect of La3+ ion-doped Co–Zn nanoferrites: structural, optical, electrical and magnetic properties. Inorg Chem Commun. 2022;146:110200. https://doi.org/10.1016/j.inoche.2022.110200.
- 25. Yang Y, Zhao M, Lai L. Surface activity, micellization, and application of nano-surfactants-amphiphilic carbon dots. Carbon. 2023;202:398–413. https://doi.org/10.1016/j.carbon.2022.11.012.
- 26.Kalaiselvan CR, Laha SS, Somvanshi SB, Tabish TA, Thorat ND, Sahu NK. Manganese ferrite (MnFe<sub>2</sub>O<sub>4</sub>) nanostructures for cancer theranostics. Coord Chem Rev. 2022;473:214809. https://doi.org/10.1016/j.ccr.2022.214809.
- 27. Kumar SR, Priya GV, Aruna B, Raju MK, Parajuli D, Murali N, Verma R, Batoo KM, Kumar R, Narayana PL. Influence of Nd3+ substituted Co0.5Ni0.5Fe<sub>2</sub>O<sub>4</sub> ferrite on structural, morphological, DC electrical resistivity and magnetic properties. Inorg Chem Commun. 2022;136:109132. https://doi.org/10.1016/j.inoche.2021.109132.
- 28. Kumari PS, Charan GV, Kumar DR. Synthesis, structural, photocatalytic and anticancer activity of Zn-doped Ni nanochromites by citrate gel auto-combustion method. Inorg Chem Commun. 2022;139:109393. <a href="https://doi.org/10.1016/j.inoche.2022.109393">https://doi.org/10.1016/j.inoche.2022.109393</a>
- 29. Kumar DR, Lincoln CA, Charan GV, Thara G, Ravinder D, Veeraswamy M, Naresh P. Study of photocatalytical, antimicrobial activity, dielectric and AC impedance properties of Zn-doped Mg nanoferrites synthesized from citrate gel auto-combustion method. Mater Chem Phys. 2022;278:125648. https://doi.org/10.1016/j.matchemphys.2021.125648
- 30.Komali C, Murali N, Rajkumar K, Ramakrishna A, Yonatan Mulushoa S, Parajuli D, Pramila Rani PN, Ampolu S, Chandra Mouli K, Ramakrishna Y. Probing the DC electrical resistivity and magnetic properties of mixed metal oxides Cr3+ substituted Mg–Zn ferrites. Chem Pap. 2023;77(1):109–117. https://doi.org/10.1007/s11696-022-02466-9
- 31.Zhang X, Mei Y, Cheng H, Ma J, Zhu F, Komarneni S. Activation of K<sub>2</sub>S<sub>2</sub>O<sub>8</sub> by Ni–Ce composite oxides for the degradation of orange II with visible light assistance. Mater Chem Phys. 2021;270:124784. https://doi.org/10.1016/j.matchemphys.2021.124784.